Multidiscipline Modeling in Materials and Structures

Experiment-based validation and uncertainty quantification of coupled multi-scale plasticity models

Garrison Stevens Sez Atamturktur Ricardo Lebensohn George Kaschner

Experiment-based validation and uncertainty quantification of coupled multi-scale plasticity models

Garrison Stevens and Sez Atamturktur
Glenn Department of Civil Engineering, Clemson University, Clemson, South Carolina, USA, and
Ricardo Lebensohn and George Kaschner
Los Alamos National Laboratory, Los Alamos, New Mexico, USA

Received 22 April 2015
Revised 17 August 2015
Accepted 10 October 2015

Abstract

Purpose – Highly anisotropic zirconium is a material used in the cladding of nuclear fuel rods, ensuring containment of the radioactive material within. The complex material structure of anisotropic zirconium requires model developers to replicate not only the macro-scale stresses but also the meso-scale material behavior as the crystal structure evolves; leading to strongly coupled multi-scale plasticity models. Such strongly coupled models can be achieved through partitioned analysis techniques, which couple independently developed constituent models through an iterative exchange of inputs and outputs. Throughout this iterative process, biases, and uncertainties inherent within constituent model predictions are inevitably transferred between constituents either compensating for each other or accumulating during iterations. The paper aims to discuss these issues.

Design/methodology/approach – A finite element model at the macro-scale is coupled in an iterative manner with a meso-scale viscoplastic self-consistent model, where the former supplies the stress input and latter represents the changing material properties. The authors present a systematic framework for experiment-based validation taking advantage of both separate-effect experiments conducted within each constituent's domain to calibrate the constituents in their respective scales and integral-effect experiments executed within the coupled domain to test the validity of the coupled system.

Findings – This framework developed is shown to improve predictive capability of a multi-scale plasticity model of highly anisotropic zirconium.

Originality/value – For multi-scale models to be implemented to support high-consequence decisions, such as the containment of radioactive material, this transfer of biases and uncertainties must be evaluated to ensure accuracy of the predictions of the coupled model. This framework takes advantage of the transparency of partitioned analysis to reduce the accumulation of errors and uncertainties.

Keywords Bayesian inference, Uncertainty propagation, Constitutive modeling, Model-form error, Newton-Raphson

Paper type Research paper

1. Introduction

In partitioned analysis, independently developed constituent models are coupled together by exchanging inputs and outputs, typically through iterative procedures[1] (Felippa *et al.*, 2001; Rugonyi and Bathe, 2001; Larson *et al.*, 2005; Matthies *et al.*, 2006; Leiva *et al.*, 2010). Such coupling eliminates the need for strong (and occasionally unwarranted) assumptions about the interactions between multiple physical phenomena (Lieber and Wolke, 2008) and results in representations of reality more accurate and complex than the individual constituents themselves (Farajpour and Atamturktur, 2012). Coupled models developed with partitioned analysis are becoming

Multidiscipline Modeling in Materials and Structures
Vol. 12 No. 1, 2016
pp. 151-176

1573-6105
DOI 10.1108/MMMS-04-2015-0023

prevalent in solving multi-physics (Kim *et al.*, 2009) and multi-scale (Gawad *et al.*, 2008) problems due to the many advantages partitioning provides, such as the ability to exploit existing codes reducing code development costs and demands (Sorti *et al.*, 2009). Additionally, partitioned analysis renders a greater ability to solve high-complexity problems (Ibrahimbegovic *et al.*, 2004) and the ability to run parallelized simulations (Park and Felippa, 1983). Hence, strongly coupled multi-scale and multi-physics models are being increasingly used to support high-consequence decision making, such as developing public policies, establishing safety procedures, and determining legal liabilities regarding not only regular system operations but also accident scenarios.

Partitioned analysis of multiple scales is especially useful for predicting time-dependent irreversible deformation in systems containing clear separation of scales, such as creep of hexagonal close packed zirconium (Wang *et al.*, 2010). These models are necessary for understanding complex material behavior under high temperatures and stresses, such as those experienced by nuclear reactor cladding, large engine fan blades, etc. Homogenization techniques such as the classic Taylor model are not suitable for modeling the constitutive behavior of these systems (Wang *et al.*, 2010; Segurado *et al.*, 2012), since obtaining accurate representations of the system response in extreme conditions is only possible when the high anisotropy and low symmetry of the crystals is accounted for through interactions between crystals. For this purpose, finite element (FE) methods are being implemented at the macro-scale to model the elastic response of the material, while single-crystal and polycrystal models are being used to represent the meso-scale viscoplasticity taking the microstructure texture evolution into account (Delannay *et al.*, 2006; Roters *et al.*, 2010; Knezevic *et al.*, 2012).

These constituents, FE model in the macro scale and polycrystal models in the meso-scale, while elaborate, inevitably provide idealized representations of reality with inherent biases and uncertainties in each. If unaccounted for, these biases and uncertainties may propagate between constituent models via the coupling interface, compensating for each other or accumulating during iterations, ultimately resulting in inferior predictive capability in the multi-scale coupled model. The effect of biases and uncertainties can be assessed by comparing coupled model predictions to experiments of the complete system (referred to herein as integral-effect experiments); and constituent models to experiments within their respective domains (referred to herein as separate-effect experiments) (Figure 1). An important benefit of partitioned analysis is this transparency and the opportunity to exploit separate-effect experiments to

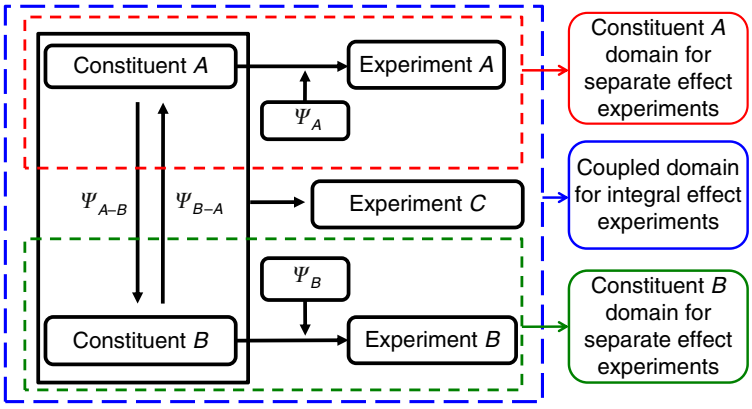

Figure 1.
Domain of separate-effect and integral-effect experiments demonstrated for a coupling problem consisting of two constituents

improve the predictive ability of individual components of a more complex, coupled model. This improvement can be accomplished in two distinct, but interconnected manners: inferring the bias in model predictions; and mitigating the uncertainty in the model parameters (Kennedy and O'Hagan, 2001; Higdon *et al.*, 2008; Farajpour and Atamturktur, 2013). Herein, these two aspects are collectively referred to as "model calibration."

In this manuscript, the authors present a framework for experiment-based model calibration and validation taking advantage of both separate- and integral-effect experiments. The approach is demonstrated on the simulation of elasto-viscoplastic material behavior of metallic specimens achieved by coupling a FE model in the macro-scale and a self-consistent homogenization of polycrystalline behavior in the meso-scale. The macro-scale FE model is imbedded with a meso-scale viscoplastic self-consistent (VPSC) model at each integration point. The VPSC model updates material properties, such as crystal structure, at each time step as the macro-scale model is deformed (Knezevic *et al.*, 2012). Error and uncertainty in the coupled model are mitigated through model calibration at the meso-scale, where parameter calibration and inference of model bias are completed using separate-effect experiments involving the loading curve of a sample of zirconium material from a uniaxial tension-compression test. Bias of the VPSC predictions is then corrected accordingly during each coupling iteration. Model validation is carried out at the macro-scale in that the predictions obtained through bias-corrected coupling process are compared against integral-effect experiments that involve the deformation of a highly anisotropic zirconium bar under a four-point bending load. This validation step demonstrates the capability of the proposed treatment of model calibration in partitioned models to yield improved accuracy in coupled model predictions.

This paper is organized as follows. In Section 2, the authors provide motivation for the management of bias and uncertainty in partitioned models accompanied by background discussion on the general framework of partitioned analysis. Next, an overview of state-of-the-art for calibration and validation of coupled models is presented in Section 3. The framework for experiment-based calibration and validation of coupled models advocated herein, which utilizes both separate- and integral-effect experiments, is discussed in detail in Section 4. Section 5 introduces the meso- and macro-scale constituent models (VPSC and FE models) as well as the associated coupling process for the case study application. The experimental campaign and numerical model development for the zirconium case study are presented in Section 6. The methodology is implemented in Section 7 for calibration and bias correction of strongly coupled VPSC-ABAQUS model for zirconium material. Finally, concluding remarks and key takeaways from the study are presented in Section 8.

2. Bias and uncertainty in coupled models

During coupling iterations, not only the constituent model predictions but also their bias and uncertainty flow back and forth between the partitioned domains[2], as illustrated in Figure 2. Uncertainty in constituent model parameters (θ in Figure 2) causes variability in the coupled model predictions (Figure 2(a)), while bias in constituent model predictions (ψ_A and ψ_B in Figure 2) results in deviations from truth (Figure 2(b)). Occurring together, these biases and uncertainties may accumulate or compensate for each other quickly becoming highly complex and difficult to trace (Rizzi *et al.*, 2012; Liang *et al.*, 2015). The choice of coupling algorithm also influences the solutions as each algorithm passes biases and uncertainties in a different manner

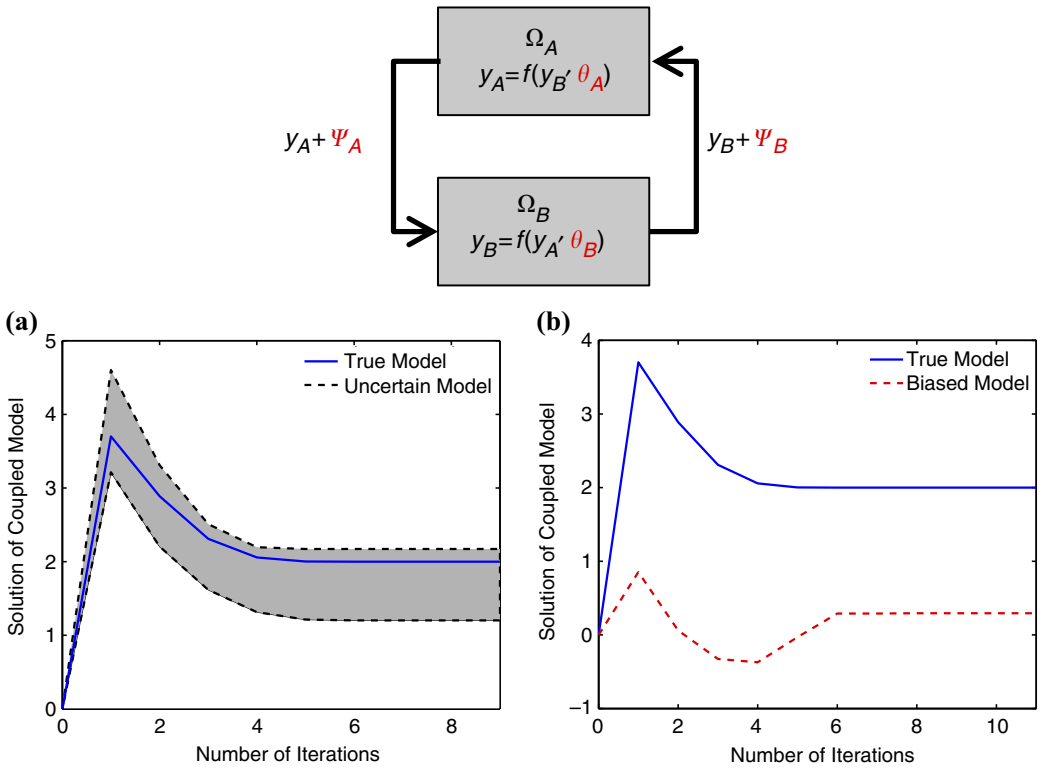

Figure 2.
Convergence of coupled model predictions to incorrect solutions due to (a) parametric uncertainty and (b) systematic bias

ultimately resulting in convergence to different solutions (Kim *et al.*, 2009) all of which may appear physically credible. Figure 2 demonstrates the effects of these biases and uncertainties on coupled model predictions in an isolated manner. Real systems, however, experience the degrading effects of both simultaneously.

The propagation of these biases and uncertainties between constituents can cause the coupling iterations to diverge or worse, converge to an incorrect solution as demonstrated in Figure 2. Such inaccurate convergence is particularly worrisome, as it may make the solution appear plausible, giving false confidence to the model developers about inaccurate scientific findings (Kim *et al.*, 2009). Such inaccurate convergence has been observed in several applications in engineering and science (Döscher *et al.*, 2002; Estep *et al.*, 2008; Kim *et al.*, 2009; Bunya *et al.*, 2010; Dietrich *et al.*, 2010; Kumar and Ghoniem, 2012a). Döscher *et al.* (2002), for instance, noted the convergence of a coupled atmosphere-ocean model to incorrect sea ice area calculations. The authors attributed this inaccurate convergence to bias in heat fluxes originating from the atmospheric model, as the stand-alone ocean model with heat flux inputs from experimental data rather than the atmospheric model produced better agreement with sea ice area measurements. Kumar and Ghoniem (2012a) recognized bias in the predictions of a coupled flow gasification model not only due to bias in the constituent flow model, but also insufficient information being passed (i.e. missing parameters) from the flow solver to the particle dispersion model, referred to herein as interface bias (Ψ_{A-B} and Ψ_{B-A} in Figure 1).

Although biases and uncertainties inherent in constituent models are of a concern for partitioned models, partitioning provides a unique transparency for their assessment and mitigation. This transparency is due to the fact that variables shared to couple the constituent models can be evaluated as outputs at the constituent levels prior to coupling.

Therefore, the transparency of partitioned models enables us to exploit separate-effect experiments conducted within each domain to calibrate the constituent models. The greatest advantage of partitioned analysis in the context of model calibration and validation is arguably its ability to exploit separate-effect experiments that are often more economical, less time-consuming and more feasible to conduct.

Figure 3 is a notional representation of the information flow as well as essential variables of a partitioned model. In this figure, control parameters, x, define the operational state of the system and are often known by both the experimentalist and model developer; calibration parameters, θ, are those that are influential in model predictions but whose exact values are uncertain and thus require calibration; and remaining input parameters, z, are those that are necessary for operating the model but are neither control nor calibration parameters. As shown in this figure, constituents may have two basic types of inputs, dependent and independent. The dependent parameters (dep in Figure 3) are the inputs to a constituent model that are dependent upon another constituent's output. Without coupling, these dependent parameters are unknown to the model developer, thus requiring assumptions to be made regarding their values. In addition, each constituent model may have independent parameters (*ind* in Figure 3), which are required for executing the constituent model but are not a function of another constituent's output and thus, are simply specified by the model developer. Control parameter, x, may be independent (meaning it is known for a model) or dependent (meaning it is unknown and must be predicted by another model). Similarly, z, can be either independent or dependent parameters. If the dependent parameter becomes a control parameter, x, for another constituent model, the propagation of uncertainty tends to be of higher concern than if the dependent output is simply defining a system property, z (Haydon and Deletic, 2009). In our framework, calibration parameters are those which are poorly known but do not depend on another model's output. Hence, according to our definition, calibration parameters are by default independent parameters.

In a similar manner, constituents may have two types of outputs, once again dependent and independent. Dependent outputs, y^{dep}, are those that become an input for another constituent, previously referred to as dependent parameters. Independent outputs, y^{ind}, are those that are not transferred to other constituents. Separate and integral-effect experiments can be conducted to observe either of these outputs, resulting in a variety of options for model calibration. For instance, one may focus on mitigating the uncertainty in calibration parameters, θ, in any one of the constituent

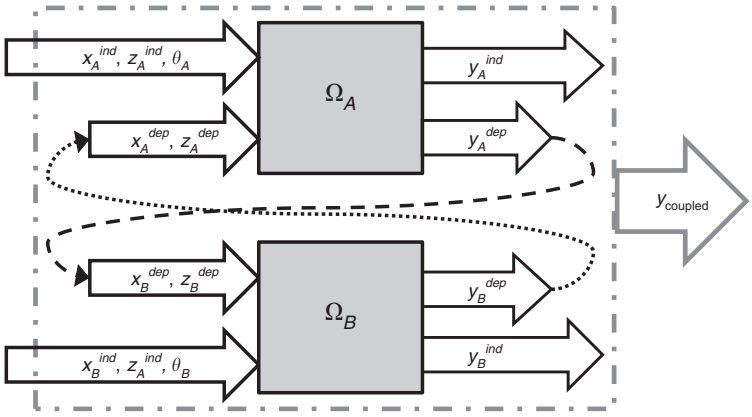

Figure 3.
Partitioned model with independent and dependent model parameters

models using either separate- or integral-effect experiments that measure dependent or independent outputs. However, it is only when separate-effect experiments observing the dependent outputs are implemented, that one can quantify the propagation of uncertainty between models as well as determine the bias associated with constituent model predictions which will be passed during coupling iterations. If such separate-effect experiments are available, then correcting for said bias before it is transferred to the next constituent becomes possible.

3. Background perspectives

In calibrating constituent models against separate-effect experiments prior to coupling, the nature of calibration that can take place can be determined based on the types of experiments available (independent or dependent). Separate-effect experiments measuring y^{ind} enable the calibration of poorly known parameters. One such example is discussed by Liu and Muraleetharan (2012) where several experimental techniques for capturing separate-effect behavior relative to several outputs of the system are implemented for calibrating constituent model parameters. Separate-effect experiments measuring dependent outputs, y^{dep}, on the other hand enables the evaluation of uncertainties as well as biases in the constituent model predictions that are passed to other constituents (Stevens and Atamturktur, 2015). Kumar and Ghoniem (2012a) took advantage of separate-effect experiments of dependent outputs, but the information gained from these was limited to tracking the propagation of uncertainties through the coupling process rather than remedying the degrading effects of this propagation. Farajpour and Atamturktur (2014) proposed an integrated coupling-uncertainty quantification framework in which constituent model parameters were calibrated and bias was quantified using separate-effect experiments. However, their study only considered bias for the purpose of avoiding compensation for said bias by uncertain parameters during calibration. Oliver *et al.* (2015) discuss the importance of not only quantifying and tracking the propagation of bias and uncertainty in constituent models, but also correcting for these factors at the constituent level, as they will affect responses of the coupled system.

Partitioned models can also be calibrated against integral-effect experiments. Earlier studies have implemented integral-effect experiments for the calibration of independent parameters in constituent models (Lin and Yim, 2006) as well as calibration of independent parameters specifically related to coupling, in that these parameters feed into both models (Liu and Muraleetharan, 2012). Using integral-effect experiments, Farajpour and Atamturktur (2014) illustrated the importance of considering both bias and uncertainty in constituent model calibration by training a discrepancy model using integral-effect experiments to bias-correct the coupled predictions. Integral-effect experiments are also highly valuable for validation of the coupled model as the coupled domain is where predictions critical for decision making will occur (Avramova and Ivanov, 2010; Kumar and Ghoniem, 2012b; Liu and Muraleetharan, 2012). Korzekwa (2009) emphasizes the fact that validation of complex models is important, as models of such complex systems often include components that cannot be accurately modeled, despite efforts to reduce assumptions through coupling. While validation of the coupled model through integral-effect experiments is necessary, engineers are often faced with the challenge of validation data at the coupled level being limited or unavailable (Kumar and Ghoniem, 2012b; Tawhai and Bates, 2011). However, bias correction of constituents throughout the coupling process using separate-effect experimental data combined with integral-effect experimental data for validation is to our knowledge yet to be explored.

4. Methodological approach

This study presents a framework for bias-corrected partitioned analysis, which begins with model calibration of uncertain parameters and inference of model bias completed within the constituent domain using separate-effect experiments. The application herein relies upon the Bayesian approach of Kennedy and O'Hagan (2001) and Higdon *et al.* (2008) for quantifying model bias. However, the framework for bias-corrected partitioned analysis is not constrained to the Bayesian approach. Rather, the method by which this bias is quantified is inconsequential to the way in which bias-corrected partitioned analysis of said bias is applied to the prediction, and as such the method selected for computer experiments. What is important, however, is the accuracy with which the method for quantifying bias is able to train the discrepancy function (Stevens and Atamturktur, 2015) as well as assessing the calibration of parameters and inference of bias in a connected manner (Farajpour and Atamturktur, 2014). A variety of methods are available for inferring bias in the constituents, starting with regression-based approaches directly relating bias to tested control settings, be they as simple linear functions (Derber and Wu, 1998), high degree polynomials where coefficients are determined stochastically (Steinberg, 1985), up to non-parametric fits such as a Gaussian process model (Sacks *et al.*, 1989; Kennedy and O'Hagan, 2001; Bayarri *et al.*, 2007), and continuing away to methods for determining relationships between discrepancy and control settings such as a maximum likelihood estimation of parameter distribution characteristics (Xiong *et al.*, 2009; Atamturktur *et al.*, 2015b) or a copula-based approach (Xi *et al.*, 2014).

4.1 Constituent model calibration

Consider the forward operator of a real physical process given by $\zeta(\boldsymbol{x})$, where $\boldsymbol{x}$ represents the control parameter settings that define the domain of applicability of the problem. Experimental measurements, $y(\boldsymbol{x})$, conducted at a number of settings, n, are our primary means to observe *reality*, but are noisy representations of the true responses generated by the process $\zeta(\boldsymbol{x})$. Herein, we assume all observation errors are independent and identically distributed as Gaussian, i.e. $\varepsilon \overset{iid}{\sim} N(0, \sigma^2)$. Experimental measurements are related to the real process by:

$$y(\boldsymbol{x}^i) = \zeta(\boldsymbol{x}^i) + \varepsilon(\boldsymbol{x}^i), \quad i = 1, \ldots, n \tag{1}$$

In developing a numerical model, η, to mimic the process $\zeta(\boldsymbol{x})$ within the domain of applicability, two essential and intertwined aspects of the model must be defined. The first of these involves a series of assumptions representing the mechanistic principles invoked to establish a link between control parameters, $\boldsymbol{x}$ and model output; and the second entails unknown (or poorly known) parameters, $\boldsymbol{\theta}$, whose meanings are associated with the chosen mechanistic principles. The unknown parameter space is explored by sampling the numerical model with specified input values, $\boldsymbol{t}$, thus generating a collection of simulations, where m represents the number of simulations:

$$\eta(\boldsymbol{x}^j, \boldsymbol{t}^j), \quad j = 1, \ldots, m \tag{2}$$

Assessing the process in a Bayesian context requires sampling the parameter distributions by executing the model with different parameter sets $(\boldsymbol{x}, \boldsymbol{t})$. Markov chain Monte Carlo (MCMC) is commonly used to explore the parameter domain as this sampling, especially implemented with Metropolis Hastings algorithm, is well suited for sampling an arbitrary distribution (Smith and Roberts, 1993; Beck and Au, 2002).

However, MCMC sampling requires a large number of simulation runs, m, which may not be feasible for problems in which the numerical model, η, is computationally demanding. Higdon *et al.* (2008) suggested the use of a Gaussian process model (GPM) when computational demands of the numerical model exceed reasonable means for MCMC sampling. A GPM is defined by a mean and covariance function, which relates all input settings throughout the model (Williams, 1998; Rasmussen, 2004; Williams and Rasmussen, 2006; Santner *et al.*, 2013). By controlling the form of this covariance, one can implement a representation of the model with desired smoothness throughout the domain of applicability. In this study, the model GPM is defined by a constant mean and a power exponential covariance as shown in the following equation, where λ_η and ρ_η are hyperparameters of the GPM to be trained:

$$\mathrm{Cov}((\mathbf{x},\mathbf{t}),(\mathbf{x}',\mathbf{t}')) = \frac{1}{\lambda_\eta}\prod_{k=1}^{p_x}\rho_{\eta k}^{4\left(x_k-x'_k\right)^2} \times \prod_{k=1}^{p_t}\left(\rho_{\eta k+p_x+k}\right)^{4\left(t_k-t'_k\right)^2} \tag{3}$$

Idealizations in the definition of the mechanistic principles causes biases in the model's output. Bias can be considered to be a model's fundamental inability to replicate reality due to incomplete representation of underlying physics or engineering principles and may originate from missing input parameters; missing or incorrectly defined relationships between control parameters and input parameters; or missing or incorrectly defined relationships between input parameters. If biases are unaccounted for during calibration, the parameters may be adjusted to values that mask the presence of model error (Kennedy and O'Hagan, 2001; Higdon *et al.*, 2008; Gaganis, 2009; Atamturktur *et al.*, 2014; Farajpour and Atamturktur, 2013). As suggested by Kennedy and O'Hagan (2001), we implement an additive approach in which the real physical process $\zeta(\boldsymbol{x})$ is related to the numerical model with best estimate parameter values, $\boldsymbol{\theta}$ by:

$$\zeta\left(\boldsymbol{x}^i\right) = \eta\left(\boldsymbol{x}^i,\boldsymbol{\theta}\right) + \psi\left(\boldsymbol{x}^i\right), \quad i = 1, \ldots, n \tag{4}$$

where $\eta(\boldsymbol{x}^i, \boldsymbol{\theta})$ is the model outputs and $\psi(\boldsymbol{x}^i)$ is the model bias at each tested setting, i and n is the number of experiments. Note that information regarding systematic bias is only available at control parameter settings where experiments have been conducted, $\boldsymbol{x}^i$. Hence estimating the bias for all other control settings, $\boldsymbol{x}$ requires that an independent model is trained. This independent model, $\delta(\boldsymbol{x})$ is henceforth referred to as "discrepancy." There is likely to be limited information, if any, about the functional form of $\delta(\boldsymbol{x})$. Kennedy and O'Hagan (2001) suggested modeling the discrepancy using a non-parametric stationary Gaussian process in order to eliminate the need for potentially strong assumptions regarding its model form. We can represent the discrepancy over the domain of applicability (Higdon *et al.*, 2008), once again using a zero mean GPM with a covariance function (shown in Equation (5)) which maintains a smooth, differentiable model fit throughout the domain. In this covariance function, λ_δ and ρ_δ are hyperparameters of the GPM to be calibrated:

$$\mathrm{Cov}\left(\mathbf{x},\mathbf{x}'\right) = \frac{1}{\lambda_\delta}\prod_{k=1}^{p_x}\rho_{\delta k}^{4\left(x_k-x'_k\right)^2} \tag{5}$$

Now that all sources of uncertainties have been defined, we can relate the numerical model predictions using best estimate parameters, $\eta(\boldsymbol{x}, \boldsymbol{\theta})$, and the discrepancy

function, $\delta(\boldsymbol{x})$, to experimental measurements at selected control settings, i, while also taking experimental error, $\varepsilon(\boldsymbol{x})$, into consideration, as shown in Equation (6):

$$y(\boldsymbol{x}^i) = \eta(\boldsymbol{x}^i, \boldsymbol{\theta}) + \delta(\boldsymbol{x}^i) + \varepsilon(\boldsymbol{x}^i) \quad i = 1, \ldots, n \tag{6}$$

Missing physics in the constituent model is corrected for through the discrepancy function, $\delta(\boldsymbol{x})$, which is trained to be an estimate of the model-form error, $\psi(\boldsymbol{x})$. This process of correcting for the inadequacy in the constituent model, referred to as "bias correction," is implemented to ultimately improve predictions of the coupled model. Determination of the discrepancy function and calibration parameter values with relation to each other prevents unwarranted compensations between parameters, which may otherwise mask model bias (Kennedy and O'Hagan, 2001; Higdon *et al.*, 2008; Farajpour and Atamturktur, 2014; Stevens and Atamturktur, 2015). Approaching this problem in the Bayesian context allows for calibration of the uncertain parameters and discrepancy function simultaneously, while also providing a smooth incorporation of the experimental errors in the calibration. This is done by simultaneously inferring distributions for uncertain parameters, as well as the numerical model GPM hyperparameters and discrepancy model hyperparameters, conditioned upon a vector of sampled model outputs, $\eta(\boldsymbol{x}, \boldsymbol{t})$, and experimental data. Once the model is calibrated at the constituent level, conditioned upon separate-effect experiments, the discrepancy function can be implemented in an iterative manner to correct the constituent model through bias-corrected partitioned analysis.

4.2 Bias-corrected partitioned analysis

In partitioned analysis, errors in constituents combine in a complex manner due to the iterative nature of the coupling iterations, making it difficult to trace the effects of constituent bias on the coupled model predictions. Partitioning allows for the calibration and bias correction of constituent models using separate-effect experiments through two unique approaches. The first of these (Figure 4(a)) involves coupling constituent models followed by calibrating their output to separate-effect experiments (see Farajpour and Atamturktur, 2014 for a demonstration of this approach). Herein, we propose a new framework referred to as "bias-corrected partitioned analysis," which operates by first calibrating and bias correcting constituent models with respect to their respective separate-effect experiments following coupling the models in a second step (Figure 4(b)).

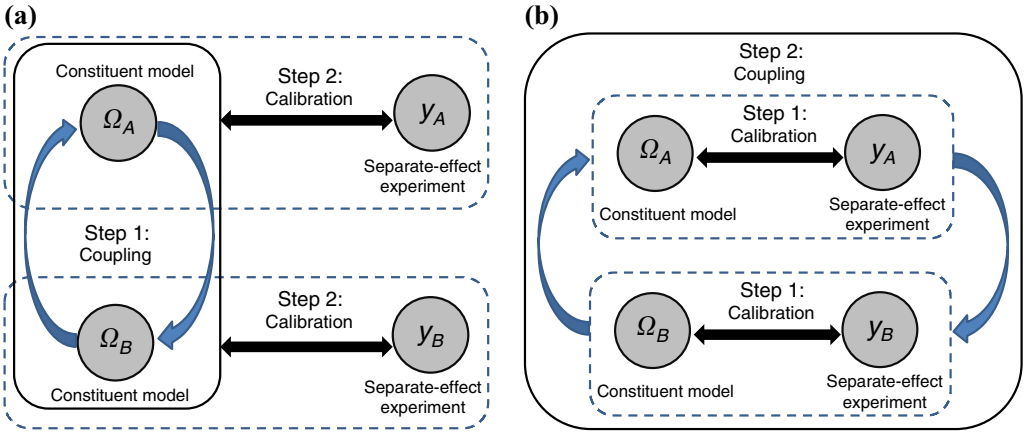

Figure 4.
Integration of coupling and model calibration using separate-effect experiments

This second framework has the advantage of reducing uncertainties and correcting for bias before they are allowed to spread throughout the coupling process and contaminate the coupled model predictions (which are typically what is used for decision making). As a final step, validation is completed for the coupled domain using the integral-effect experiments. While this manuscript focusses on the correction of constituent models, the framework may also be expanded to correct for interface bias (recall Ψ_{A-B} in Figure 1), should appropriate integral-effect experiments be available. Interface bias is introduced due to omitted or misrepresented relationships between constituents. These improperly defined relationships may be due to missing dependent parameters that should be transferred between models.

4.3 Conceptual demonstration of bias-corrected partitioned analysis

Consider two models representative of two domains (Ω_A and Ω_B) coupled through the iterative exchange of outputs using a Newton-Raphson scheme (as shown in Figure 6). Let us take Ω_B as a biased model and Ω_A as a bias-free model. Figure 5(a) illustrates the biased predictions of Ω_B compared to a rich set of separate-effect experiments (our closest representation of truth). Here, we train a discrepancy function (dashed line shown in Figure 5(b)) using the bias inferred at tested settings (stars shown in Figure 5(b)).

Note in Figure 5(b) that the discrepancy is defined for all values of x_B, control parameter for Ω_B. This discrepancy function is used to correct the predictions of Ω_B, which serves as a dependent input parameter for Ω_A. In each iteration, the predictions of Ω_B are corrected by the value corresponding to the given x_B in the discrepancy function (Figure 6). Once this bias correction is applied concurrently with the coupling scheme, predictions of the coupled model are improved. Here, the coupled predictions

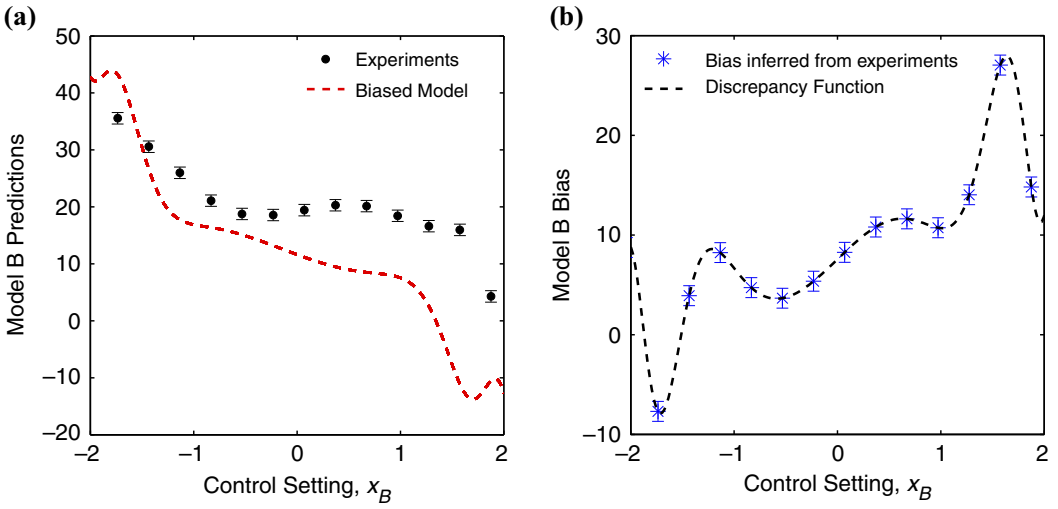

Figure 5.
(a) Stand-alone Ω_B model predictions compared and relative separate-effect experiments and (b) bias inferred at experimental measurement points and discrepancy trained throughout the model domain

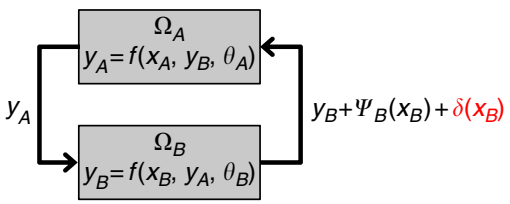

Figure 6.
Illustration of bias-corrected partitioned analysis

are made in the domain of Ω_A, but require iterations between the models. A few important observations may be garnered from Figure 7. First, the coupled predictions shown for the domain of Ω_A are altered due to the bias in Ω_B, even though Ω_A was an initially correct model. Hence, the degrading effect of bias is not limited to the domain in which it originates. Rather, much like an infectious disease, the constituent bias makes its way through the coupling interface to diminish predictive capabilities in the other domain. Second, in our academic example, bias correction of Ω_B at every iteration in the coupled model almost completely accounts for inaccuracies in the constituent and recovers a significant amount of error in the coupled model, bringing predictions of the coupled model to less than 1 percent error, in comparison to the 15 percent error prior to bias correction.

5. Meso- and macro-scale coupling of VPSC and ABAQUS FE codes

5.1 Meso-scale VPSC code

The VPSC code, developed by Lebensohn and Tomé (1993), predicts the texture evolution of highly anisotropic polycrystalline material. VPSC operates under the assumption that a polycrystalline material can be represented by a set of orientations of individual single-crystal grains, each of which can then be treated as an inhomogeneity embedded within a homogeneous effective medium. With this assumption, interaction equations are formulated to linearly relate the stress and strain rate of a single grain to the stress and strain rate of the surrounding effective medium. The VPSC formulation uses an integral approach to update the grain shape effect and evolution of the polycrystal orientations with deformation, enabling the prediction of texture evolution for the metallic materials. Applying viscoplastic deformation, the stress-strain response and microstructure evolution are predicted at the single crystal using the following constitutive relationship (Tomé *et al.*, 2001):

$$\dot{\varepsilon}_{vp} = \dot{\gamma}_o \sum_s m_{ij}^s \left(\frac{m^s : \sigma'}{\tau^s} \right)^n \tag{7}$$

where s is the number of active slip and twinning systems, n the inverse of the rate sensitivity, τ^s the threshold shear stress, m^s the Schmid tensor, $\boldsymbol{\sigma}'$ is the Cauchy stress

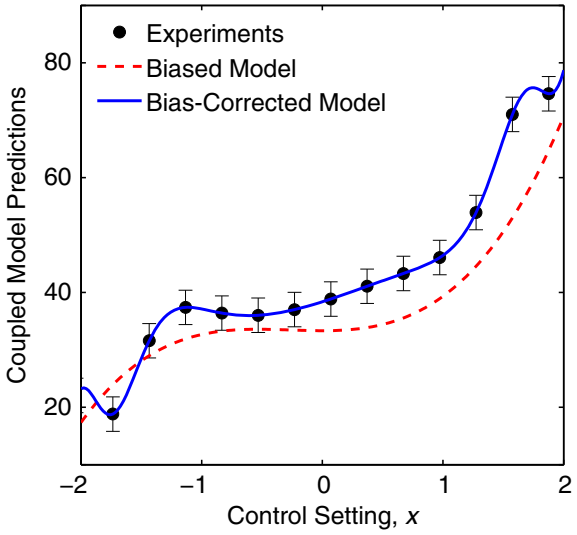

Figure 7.
Improvement in coupled model predictions achieved through bias-corrected partitioned analysis

deviator, and $\dot{\boldsymbol{\varepsilon}}_{vp}$ the viscoplastic strain-rate. The threshold shear stress, $\boldsymbol{\tau}^s$ in Equation (7) is affected by the deformation modes active during hardening. A reference hardening function is defined by:

$$\tau^s = \tau_0^s + \left(\tau_1^s + \theta_1^s \Gamma\right)\left(1 - exp\left(-\frac{\theta_0^s \Gamma}{\tau_1^s}\right)\right) \tag{8}$$

where τ_0^s, θ_0^s, θ_1^s, and $\tau_0^s + \tau_1^s$ are the initial critical resolved shear stress (CRSS), initial hardening rate, asymptotic hardening rate, and back-extrapolated CRSS, respectively. Each of these parameters takes a different value for each active deformation system. Anisotropic zirconium at room temperature has three active slip and twinning modes (prismatic, pyramidal, and tensile twinning) each with a hardening function of its own containing the four hardening parameters. These hardening parameters are poorly known and thus must be calibrated against physical experiments.

5.2 Macro-scale ABAQUS code

At the macro-scale, ABAQUS calculates the total strain increment, $\Delta\boldsymbol{\varepsilon}$, which can be partitioned into elastic, $\Delta\boldsymbol{\varepsilon}_{el}$, and viscoplastic, $\Delta\boldsymbol{\varepsilon}_{vp}$ components:

$$\Delta\boldsymbol{\varepsilon} = \Delta\boldsymbol{\varepsilon}_{el} + \Delta\boldsymbol{\varepsilon}_{vp} = \boldsymbol{C}^{-1} : \Delta\boldsymbol{\sigma} + \Delta\boldsymbol{\varepsilon}_{vp}(\boldsymbol{\sigma}) \tag{9}$$

For each iteration at a given strain increment, $\Delta\boldsymbol{\varepsilon}$, the stress increment, $\Delta\boldsymbol{\sigma}$ is determined:

$$\Delta\boldsymbol{\sigma} = \boldsymbol{\sigma}^{t+\Delta t} - \boldsymbol{\sigma}^t \tag{10}$$

5.3 Coupling between VPSC and ABAQUS

Using a Newton-Raphson iterative scheme, the VPSC and ABAQUS codes are coupled with the following convergence criteria $X(\Delta\boldsymbol{\sigma}) = 10^{-6}$ (i.e. $\Delta\boldsymbol{\varepsilon} \approx \Delta\boldsymbol{\varepsilon}^{FE}$):

$$X(\Delta\boldsymbol{\sigma}) = \Delta\boldsymbol{\varepsilon} - \Delta\boldsymbol{\varepsilon}^{FE} = \boldsymbol{C}^{-1} : \Delta\boldsymbol{\sigma} + \Delta t \dot{\boldsymbol{\varepsilon}}_{vp}^{(px)}\left(\boldsymbol{\sigma}^t + \Delta\boldsymbol{\sigma}\right) - \Delta\boldsymbol{\varepsilon}^{FE} \tag{11}$$

After convergence in stress equilibrium is reached at each time step, viscoplastic strain-rate $\dot{\boldsymbol{\varepsilon}}_{vp}$, hardening variables and crystal orientations q, and tangent stiffness matrix $\boldsymbol{C}$, are accepted for every integration point, allowing ABAQUS to repeat the iteration process at the next time step, $t + \Delta t$, with an increased displacement, $u + \Delta u$ as illustrated in Figure 8.

Coupling between the two scales occurs as the FE model provides VPSC with updated stress $\boldsymbol{\sigma}$, and VPSC provides the FE model with updated viscoplastic strain-rate, $\dot{\boldsymbol{\varepsilon}}_{vp}$, hardening variables and crystal orientations q, and tangent stiffness matrix C, as shown in Figure 8. Specifically, the VPSC model supplies a texture-sensitive constitutive relationship between stress and viscoplastic strain-rate (see Equation (7)). This constitutive relationship takes both slip and twinning between crystals into account, yielding an accurate representation of the time-dependent, irreversible deformations of the polycrystalline material (Tomé *et al.*, 2001). Figure 9 illustrates the domain of each of the models and their corresponding separate- and integral-effect experiments.

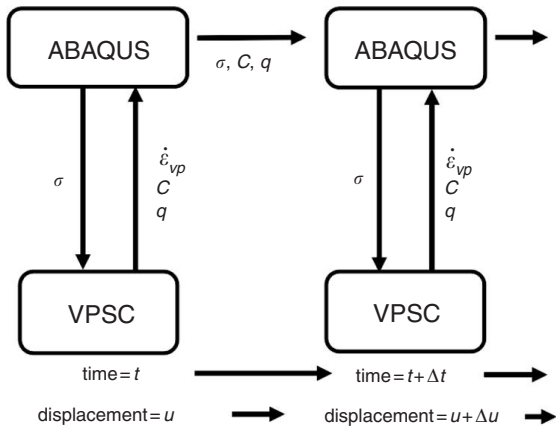

Figure 8.
VPSC-ABAQUS coupling interactions

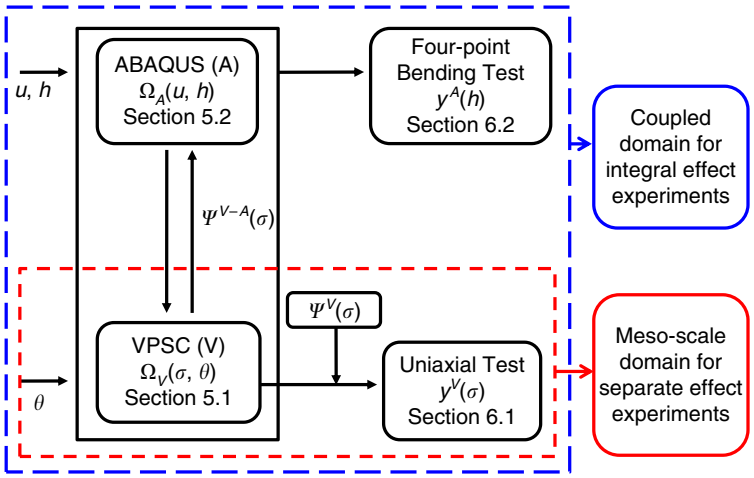

Figure 9.
Separate-effect and integral-effect experiments for the coupled VPSC-ABAQUS model for cladding materials

6. Experimental and numerical campaign

Separate-effect experimental data for calibration of the VPSC meso-scale constituent model are collected in a series of uniaxial tension-compression tests and integral-effect experimental data for validation of the coupled model are gathered from the four-point bending test of a zirconium beam. Cylinders used in the uniaxial test, as well as the beam used in the four-point bending test, are cut from a plate of zirconium processed by clock rolling and vacuum annealing processes to produce highly textured properties (Kaschner *et al.*, 2001).

6.1 Uniaxial tension and compression tests of a zirconium cylinder: separate-effect experiments and VPSC model

Uniaxial tension/compression tests are completed on cylindrical zirconium specimens to collect stress and plastic strain data for in-plane compression (IPC) and in-plane tension (IPT). Tensile specimens are cut to a nominal gauge length of 17.7 mm and a diameter of 2.25 mm; compression samples are cut to a length of 5 mm and a diameter of 5 mm. Tests are conducted at a temperature of 293 K with a strain rate of 0.001 s^{-1}. Zirconium samples are deformed up to a plastic strain of 25 percent along the testing direction (Tomé *et al.*, 2001). Loading curves for IPC and IPT collected from the experimental tests are shown in Figure 10.

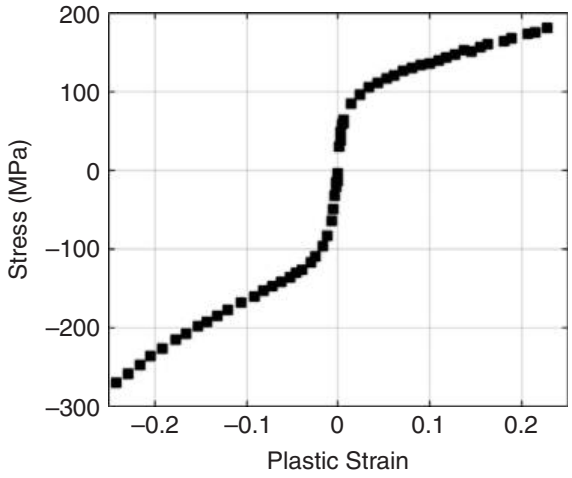

Figure 10.
Uniaxial tension and compression tests data

6.2 Four-point bending of a zirconium beam: integral-effect experiments and multi-scale FE-VPSC model

A zirconium plate is cut into beams with dimensions of $6.35 \times 6.35 \times 50.8$ mm and then vacuum encapsulated and heat treated, producing an equiaxed grain structure containing grains with a mean size of approximately 25 μm. Roller bearings and hardened steel dowel pins are placed at four locations within the frame to minimize the friction that may be produced due to large strains and high forces. Load is applied by upper pins located 6.35 mm to the left and right of the center, which are displaced 6 mm while the lower pins, located 12.7 mm from the center on both sides, remain stationary. Experiments are performed such that the nominal strain-rate at the outer fibers of the beam is $10^{-3}\,s^{-1}$ (Kaschner *et al.*, 2001).

Tests are conducted with the beam being bent parallel to the crystal axis. Prior to bending the beam is marked with a 161 point grid, composed of seven columns with 23 indentions each. Columns are spaced 1.016 mm apart and each point in the column spaced 0.254 mm apart. After bending, the displacement of these points is measured to calculate the experimental strain. Plastic strain is measured at the centerline of the beam after the maximum displacement is reached (Figure 11). The initial and final positions of the dot grid, measured using dot-matrix deposition and mapping, are used

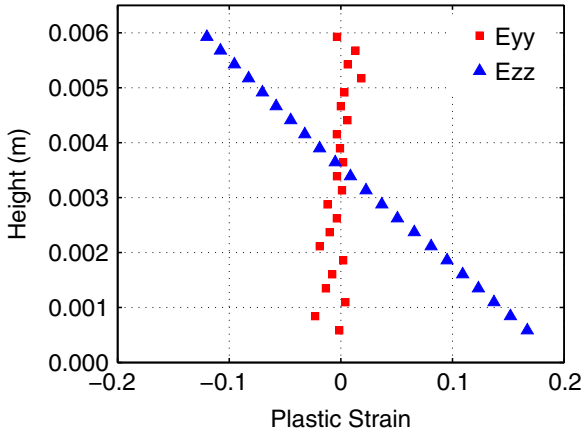

Figure 11.
Four-point bending test experimental plastic strain data

to calculate strain at each marked point of the beam face. Figure 12 highlights the dot matrix used for strain measurements on the test specimen.

The ABAQUS FE model simulating macro-scale behavior is composed of a mesh of $32 \times 4 \times 4$ C3D20R element with 20 nodes (Figure 13). The VPSC polycrystal model is integrated in the FE model using a user-defined material subroutine at every Gauss integration point (Knezevic *et al.*, 2012) as previously explained in Section 5.3.

7. Bias-corrected partitioned analysis of multi-scale plasticity model

7.1 Calibration of the VPSC model

For our application in modeling the time-dependent irreversible deformation of a zirconium beam, the stand-alone VPSC model is calibrated using separate-effect experiments, i.e. uniaxial tension and compression tests of a zirconium cylinder described earlier in Section 6.1. As illustrated in Figure 14, the control parameter is stress, $\boldsymbol{\sigma}$ at varying levels of which, the strain-rate measurements are available.

Potential parameters for calibration are the 12 hardening parameters as well as the parameter n, representing the inverse of rate sensitivity parameter, seen in Equation (7). Among these candidate parameters, appropriately selecting the parameters for calibration is critical. Here, we evaluate the sensitivity and uncertainty of parameters in a manner reminiscent to the parameter identification and ranking table Hegenderfer

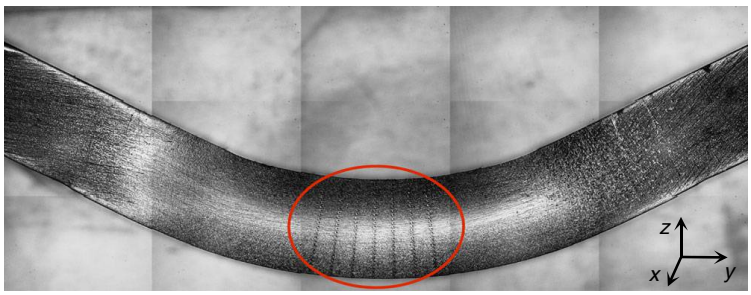

Figure 12.
Zr beam after four-point bending experiment

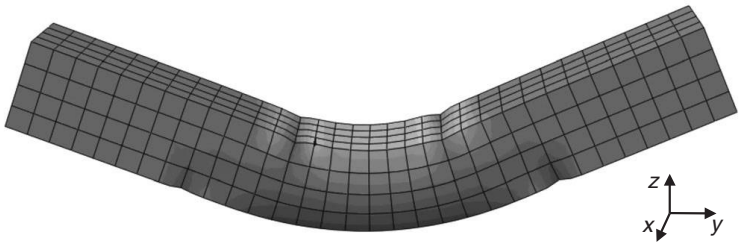

Figure 13.
Macro-scale FE model

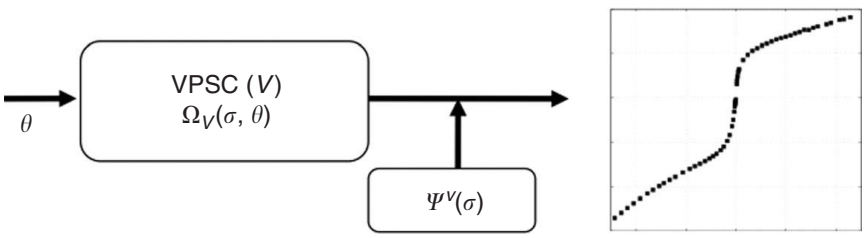

Figure 14.
Separate-effect calibration with input of polycrystal material properties, θ, into the VPSC solver and comparison of stress-plastic strain output to experimental data

and Atamturktur, 2013). A parameter that exercises little influence on the available experiments will not be properly calibrated and possibly cause ill-conditioning – on the other hand, a parameter whose value is known with little uncertainty should not be calibrated. Hence, the most logical approach is calibrating only those parameters that are sensitive to available experiments and uncertainty to the analyst. The inverse of rate sensitivity parameter, n, in Equation (7) is not only poorly known but also has been shown to be significantly influential on the VPSC model predictions of stress and texture in previous studies (Atamturktur *et al.*, 2013, 2015a, b). Hardening parameters for the threshold shear stress (Equation (8)) are also uncertain. The sensitivity of these parameters is determined through a main-effect analysis of variance test of the 12 hardening parameters. Results of the sensitivity analysis indicate τ_0, τ_1, and θ_1 in the prismatic slip system to be the main contributors to the variance in model outputs, as shown in Table I, effectively reducing the problem to the calibration of four parameters (n and prismatic τ_0, τ_1, and θ_1).

Herein, MCMC sampling is used to explore the parameter domain, drawing 10,000 samples. To reduce the computational demand of MCMC, a fast-running GPM as explained in Section 4.1 is used as an emulator in place of the VPSC model. The GPM is trained with 100 VPSC runs (50 in the tension range and 50 in the compression range) obtained using Latin hypercube sampling to ensure the parameter domain is adequately explored. Prior distributions of hyperparameters for the model GPM (Equation (5)) and discrepancy GPM (Equation (3)) proposed in Gattiker (2008) are used. Uniform prior distributions are assigned for the four calibration parameters, with upper and lower bounds as listed in Table II. Posterior distributions of the four calibration parameters are shown in Figure 15 and the main statistical properties of these posterior distributions are listed in Table II. Figure 16 illustrates the improvement obtained in the stand-alone VPSC model predictions after calibration.

7.2 Implementation of bias-corrected partitioned analysis

Mean values of the posterior distributions for uncertain parameters of the meso-scale model (Table II) are entered as the input for the coupled multi-scale VPSC-ABAQUS

Parameter	R^2 value (%)
Prismatic slip	
τ_0	41.5
τ_1	30.50
θ_0	0.60
θ_1	26.90
Tensile twinning	
τ_0	0.69
τ_1	0.32
θ_0	0.08
θ_1	0.01
Pyramidal slip	
τ_0	0.03
τ_1	0.01
θ_0	0.00
θ_1	0.01

Table I. Sensitivity analysis of VPSC model hardening parameters

model, effectively improving the agreement between coupled model predictions and integral-effect experiments as shown in Figure 18. While calibration improves the agreement to experiments, the model continues to underestimate the plastic strain particularly at the extremes of the distribution, as detailed in Table III. However, note that thus far, bias in constituent models' predictions is not accounted for. A portion of this underestimation can be explained by the discrepancy remaining between VSPC simulations and separate-effect experiments even after calibration.

	Prior		Posterior	
Parameter	Lower bound	Upper bound	Mean	SD
n	0	20	13.43	2.58
Prismatic τ_0	0	28	23.24	4.66
Prismatic τ_1	0	24	19.52	3.15
Prismatic θ_1	0	80	71.45	7.55

Table II. Prior and posterior mean for calibration parameters

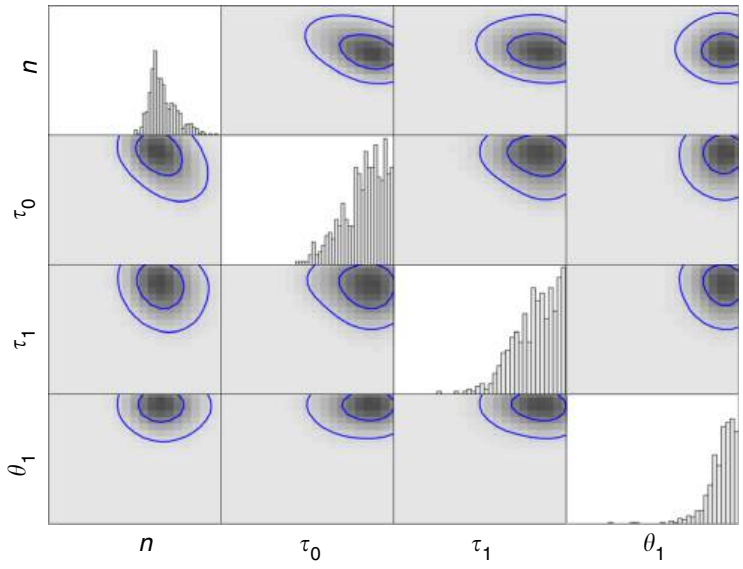

Figure 15. Posterior distributions of calibration parameters

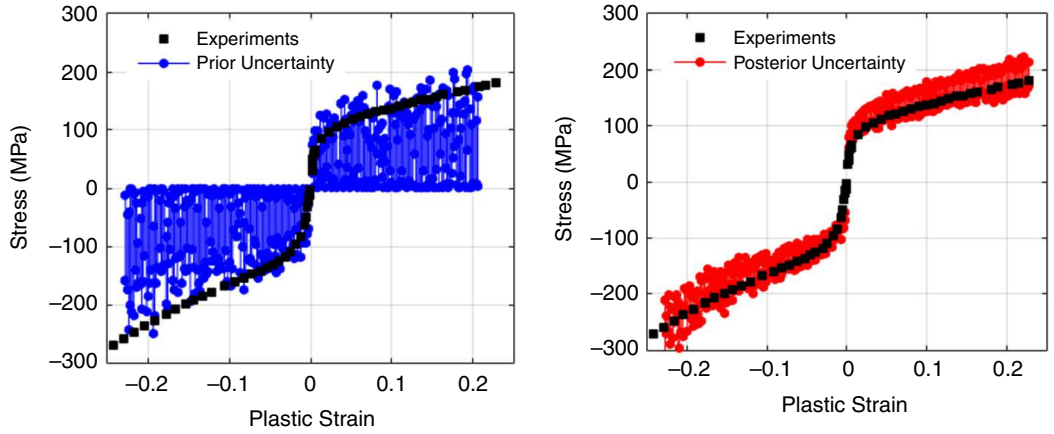

Figure 16. Stand-alone VPSC model predictions (left) prior to calibration and (right) after calibration with separate-effect uniaxial experiments

It should be noted that the separate-effect experiments available are only for the in-plane crystal orientation, which relates to a single direction of the stress and strain tensors of the numerical model. Therefore, bias correction in this study is only applied in this direction. The discrepancy model to represent this bias is inferred with stress as the control variable and plastic strain as the response feature. This inference is completed at the same time as the uncertain input parameters are calibrated through the procedure explained previously in Section 4. Discrepancy is accounted for through bias correction of the meso-scale constituent model at every iteration, such that for every calculated stress point, the corresponding plastic strain is corrected (Figure 17). The discrepancy function trained for VPSC model is used to correct plastic strain according to the stress supplied by the macro-scale ABAQUS model. In this case, a constant correction factor is applied for the tensile and compression regions, where plastic strain is increased by 40 percent in tension and decreased by 10 percent in compression. The calibrated and bias-corrected VPSC-ABAQUS model predictions are shown in Figure 18. Also shown in Figure 18 is the prediction uncertainty determined by considering the uncertainty remaining in calibrated parameters (by one standard deviation). Most notably, the bias-corrected model with mean calibration parameter values from Table II is shown to improve predictions at the maximum tensile and compressive plastic strains, which are the locations of highest concern for analyzing the failure of this system (Table III).

In this particular application, a significant limitation is the presence of multiple dependent parameters between VPSC to ABAQUS constituent models, namely, viscoplastic strain-rate, $\dot{\boldsymbol{\varepsilon}}_{vp}$, crystal and texture properties, q, and tangent stiffness

Table III. Predictions of maximum tensile and compressive plastic strains compared with experimental measurements

	Maximum plastic strain		Percent difference from experiments	
	Top of beam (compression)	Bottom of beam (tension)	Top of beam (compression) (%)	Bottom of beam (tension) (%)
Experiment	−0.148	0.194	–	–
Uncalibrated model	−0.062	0.066	81.9	98.4
Calibrated model	−0.078	0.082	61.9	81.1
Calibrated model with bias correction	−0.086	0.125	52.9	43.2

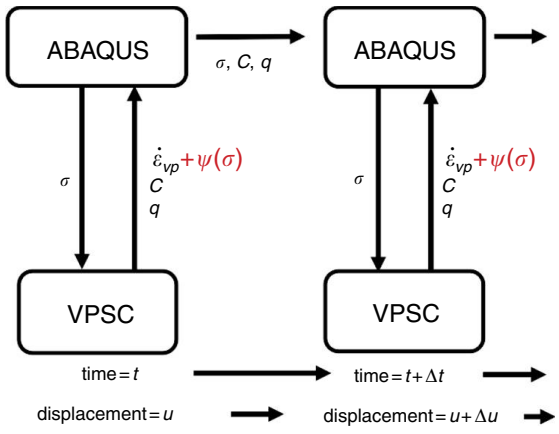

Figure 17. VPSC-ABAQUS coupling interactions with discrepancy accounted for in the meso-scale

matrix, ***C***, (recall Figure 8) and the absence of separate-effect experimental data available for each of these dependent parameters. Therefore, the other directions of the viscoplastic strain-rate tensor, as well as the crystal orientations and tangent stiffness matrix, are left uncorrected, thus limiting the extent to which the bias in constituent predictions can be remedied. Despite this limitation, the effect of partially correcting for discrepancy at the meso-scale propagates to produce improvements in the predictions of the coupled model. It is expected that if experiments were to be available for all components of the coupling, predictions would further improve and reach better agreement with experiments.

To demonstrate this aspect, consider a pair of numerical equations containing multiple dependent parameters being coupled as to represent a scenario similar to that of the VPSC-ABAQUS coupled model. As shown in Figure 19, parameters B and C are each dependent upon parameter A, which is likewise dependent upon parameters B and C. Synthetic experiments are created by using "true" values for A, B, and C, while biased simulations are created by altering the physics behind B and C. Hence, the meso-scale constituent model is taken to be biased.

Let us consider two scenarios. In the first scenario, only experiments for output B are available and in the second scenario, experiments are available for both B and C, allowing for full correction of the model. Figure 20 shows the results for the first scenario. When only B is corrected, the coupled simulation is not able to achieve

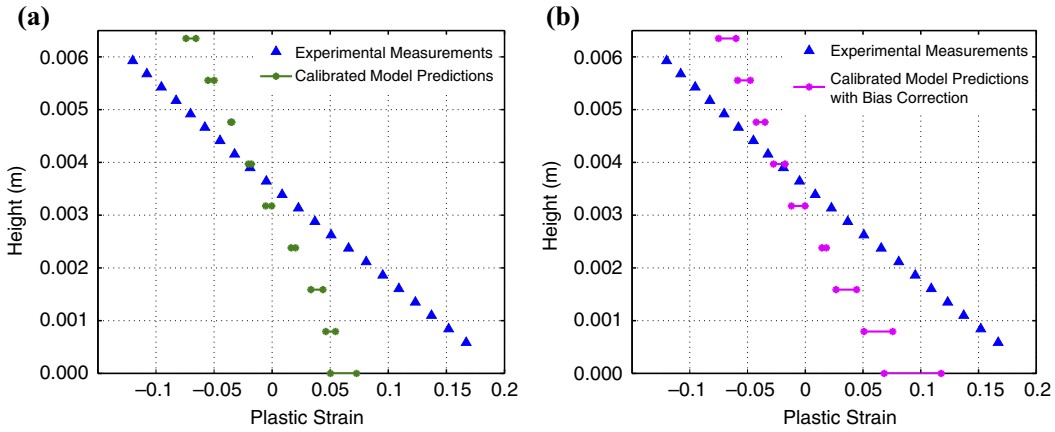

Figure 18. Results of coupled VPSC-ABAQUS model predictions (a) after VPSC model calibration but prior to bias correction and (b) after VPSC model calibration and bias correction

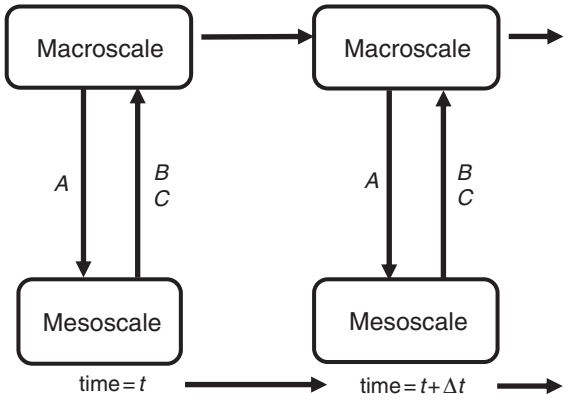

Figure 19. Example with multiple components of constituent model coupled

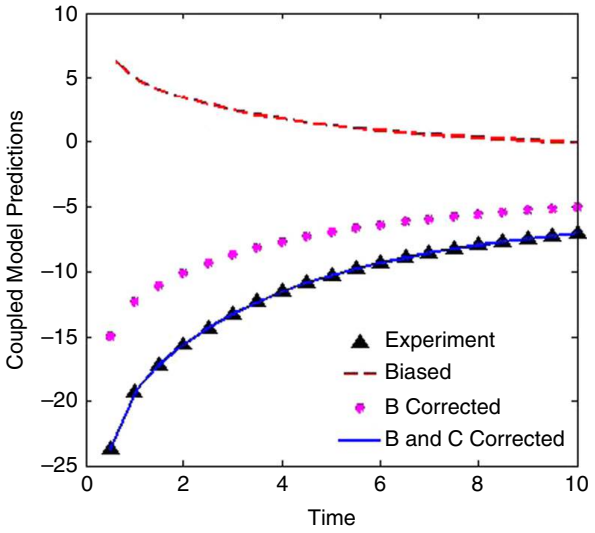

Figure 20.
Effect of only correcting one component of a constituent model

agreement with the experiments, as the average error in the coupled model predictions is only reduced, though not entirely corrected. After correcting both dependent outputs B and C, however, the simulation and experiments show improved agreement (assuming the quality and quantity of separate-effect experiments is sufficient for accurately training discrepancy).

8. Conclusion

With coupled modeling coming to the forefront of engineering practices as systems become more and more complex, a systematic framework for calibration and bias correction of partitioned models stands to make a significant impact in many engineering fields. Each constituent of a coupled model has its own unknown parameters and missing physics and engineering phenomena, resulting in bias and uncertainty that may impede the predictive capability of the coupled model, if left unaccounted for. Additionally, neglecting to account for bias during calibration may result in parameters being calibrated to incorrect values to compensate for bias.

This paper demonstrates that calibration and bias correction of the constituent-level model through the use of separate-effect experiments mitigates the accumulation of error and improves the predictive capabilities of not only the constituents, but also the coupled model. The application presented herein illustrates a real-life scenario where bias-corrected partitioned analysis utilizing separate-effect experiments improves the predictive capability of a multi-scale plasticity model. Implementation of the bias-corrected partitioned analysis paradigm allowed a 38.5 percent improvement in the fidelity of predictions for a highly anisotropic zirconium beam exposed to extreme loading. The improvement obtained in this application demonstrates the capability of the bias-corrected partitioned analysis framework to advance the predictive maturity of complex multi-scale models, therefore instilling confidence in these models as the basis for high-consequence decision making.

In complex systems, it is possible for constituent models to have multiple dependent parameters. Within the bias-corrected partitioned analysis framework, more than one dependent parameter involved in the coupling scheme requires not only sufficient quantity and quality of experiments for the constituent, but more specifically experiments related to each dependent parameter that is being transferred.

When experiments are unavailable for some of the coupled parameters, only a partial bias correction may be completed. Often times partial bias correction is better than no correction at all. This procedure, however, should be done with much caution, taking into consideration the possible consequences of neglecting to correct the other parameters.

Aside from the biases and uncertainties in the constituents themselves, the coupling process may also introduce its own spectrum of biases and uncertainties due to an inability to perfectly model the physics of coupling operations. Implications of biases and uncertainties introduced by the coupling interface have been neglected in this study, but should be investigated in future work.

Acknowledgments

This research has been performed in part using funding received from the Department of Energy Office of Nuclear Energy's Nuclear Energy University Programs (Contract Number: 00101999). The authors would like to thank Marko Knezevic of University of New Hampshire for his assistance in sharing the coupled FE-VPSC model. The technical support of Eddie Duffy of Clemson University in the use of the Palmetto Cluster is also appreciated. Finally, the editorial assistance of Godfrey Kimball of Clemson University is acknowledged.

Notes

1. Here, the term partitioned analysis (also commonly referred to as co-simulation) is used to define constituent models developed independent from each other regardless of whether their iterations advance in the same time step or not.
2. Herein "domain" is defined as the boundaries within which of each model is designed to operate (e.g. separate domains representing fluid and structure behaviors in a fluid-structure interaction problem).

References

Atamturktur, S., Hegenderfer, J., Williams, B. and Unal, C. (2015a), "Selection criterion based on an exploration-exploitation approach for optimal design of experiments", *Journal of Engineering Mechanics*, Vol. 141 No. 1, pp. 04014108-2-9.

Atamturktur, S., Liu, Z., Cogan, S. and Juang, C.H. (2014), "Calibration of imprecise and inaccurate numerical models considering fidelity and robustness: a multi-objective optimization based approach", *Structural and Multi-disciplinary Optimization*, Vol. 51 No. 3, pp. 659-671.

Atamturktur, S., Williams, B., Egeberg, M. and Unal, C. (2013), "Batch sequential design of optimal experiments for improved predictive maturity in physics-based modeling", *Structural and Multidisciplinary Optimization*, Vol. 48 No. 3, pp. 549-569.

Atamturktur, S., Hegenderfer, J., Williams, B., Egeberg, M., Lebensohn, R. and Unal, C. (2015b), "A resource allocation framework for experiment-based validation of numerical models", *Journal of Mechanics of Advanced Materials and Structures*, Vol. 22 No. 8, pp. 641-654.

Avramova, M.N. and Ivanov, K.N. (2010), "Verification, validation and uncertainty quantification in multi-physics modeling for nuclear reactor design and safety analysis", *Progress in Nuclear Energy*, Vol. 52 No. 7, pp. 601-614.

Bayarri, M.J., Berger, J.O., Paulo, R., Sacks, J., Cafeo, J.A., Cavendish, J., Lin, C. and Tu, J. (2007), "A framework for validation of computer models", *Technometrics*, Vol. 49 No. 2, pp. 138-154.

Beck, J.L. and Au, S.K. (2002), "Bayesian updating of structural models and reliability using Markov chain Monte Carlo simulation", *Journal of Engineering Mechanics*, Vol. 128 No. 4, pp. 380-391.

Bunya, S., Dietrich, J.C., Westerink, J.J., Ebersole, B.A., Smith, J.M., Atkinson, J.H., Jensen, R., Resio, D.T., Luettich, R.A., Dawson, C., Cardone, V.J., Cox, A.T., Powell, M.D., Westerink, H.J. and Roberts, H.J. (2010), "A high-resolution coupled riverine flow, tide, wind, wind wave, and storm surge model for Southern Louisiana and Mississippi. Part I: model development and validation", *Monthly Weather Review*, Vol. 138 No. 2, pp. 345-377.

Delannay, L., Jacques, P.J. and Kalidindi, S.R. (2006), "Finite element modeling of crystal plasticity with grains shaped as truncated octahedrons", *International Journal of Plasticity*, Vol. 22 No. 10, pp. 1879-1898.

Derber, J.C. and Wu, W. (1998), "The use of TOVS cloud-cleared radiances in the NCEP SSI analysis system", *Monthly Weather Review*, Vol. 126 No. 8, pp. 2287-2299.

Dietrich, J.C., Bunya, S., Westerink, J.J., Ebersole, B.A., Smith, J.M., Atkinson, J.H., Jensen, R., Resio, D.T., Luettich, R.A., Dawson, C., Cardone, V.J., Cox, A.T., Powell, M.D., Westerink, H.J. and Roberts, H.J. (2010), "A high-resolution coupled riverine flow, tide, wind, wind wave, and storm surge model for Southern Louisiana and Mississippi. Part II: synoptic description and analysis of Hurricanes Katrina and Rita", *Monthly Weather Review*, Vol. 138, pp. 378-404.

Döscher, R., Willén, U., Jones, C., Rutgersson, A., Markus Meier, H.E., Hansson, U. and Phil Graham, L. (2002), "The development of the regional coupled ocean-atmosphere model RCAO", *Boreal Environmental Research*, Vol. 7, pp. 183-192.

Estep, D., Carey, V., Ginting, V., Tavener, S. and Wildey, T. (2008), "A posteriori error analysis of multiscale operator decomposition methods for multiphysics models", *Journal of Physics: Conference Series*, Vol. 125 No. 1, pp. 1-16.

Farajpour, I. and Atamturktur, S. (2012), "Optimization-based strong coupling procedure for partitioned analysis", *ASCE Journal of Computing in Civil Engineering*, Vol. 26 No. 5, pp. 648-660.

Farajpour, I. and Atamturktur, S. (2013), "Error and uncertainty analysis of inexact and imprecise computer models", *Journal of Computing in Civil Engineering*, Vol. 27 No. 4, pp. 407-418.

Farajpour, I. and Atamturktur, S. (2014), "Partitioned analysis of coupled numerical models considering imprecise parameters and inexact models", *Journal of Computing in Civil Engineering*, Vol. 28 No. 1, pp. 145-155.

Felippa, C.A., Park, K.C. and Farhat, C. (2001), "Partitioned analysis of coupled mechanical systems", *Computer Methods in Applied Mechanics and Engineering*, Vol. 190 No. 24, pp. 3247-3270.

Gaganis, P. (2009), "Model calibration/parameter estimation techniques and conceptual model error", in Baveye, P.C., Laba, M. and Mysiak, J. (Eds), *Uncertainties in Environmental Modelling and Consequences for Policy Making*, Springer, Dordrecht, pp. 129-154.

Gattiker, J.R. (2008), "Gaussian process models for simulation analysis (GPM/SA) command, function, and data structure reference", Technical Report No. LA-UR-08-08057, Los Alamos National Laboratory, Los Alamos, NM.

Gawad, J., Niznik, B., Kuziak, R. and Pietrzyk, M. (2008), "Validation of multi-scale model describing microstructure evolution in steels", *Steel Research*, Vol. 79 No. 8, pp. 652-659.

Haydon, S. and Deletic, A. (2009), "Model output uncertainty of a coupled pathogen indicator-hydrologic catchment model due to input data uncertainty", *Environmental Modelling and Software*, Vol. 24 No. 3, pp. 322-328.

Hegenderfer, J. and Atamturktur, S. (2013), "Prioritization of code development efforts in partitioned analysis", *Computer-Aided Civil and Infrastructure Engineering*, Vol. 28 No. 4, pp. 289-306.

Higdon, D., Gattiker, J., Williams, B. and Rightlet, M. (2008), "Computer model calibration using high-dimensional output", *Journal of the American Statistical Association*, Vol. 103 No. 482, pp. 570-583.

Ibrahimbegovic, A., Knopf-Lenoir, C., Kučerová, A. and Villon, P. (2004), "Optimal design and optimal control of elastic structures undergoing finite rotations and deformations", *International Journal for Numerical Methods in Engineering*, Vol. 61 No. 14, pp. 2428-2460.

Kaschner, G.C., Bingert, J.F., Liu, C., Lovato, M.L., Maudlin, P.J., Stout, M.G. and Tomé, C.N. (2001), "Mechanical response of zirconium – II. experimental and finite element analysis of bent beam", *Acta Materialia*, Vol. 49 No. 15, pp. 3097-3108.

Kennedy, M.C. and O'Hagan, A. (2001), "Bayesian calibration of computer models", *Journal of the Royal Statistical Society (Ser. B)*, Vol. 63 No. 3, pp. 425-464.

Kim, J., Tchelepi, H.A. and Juanes, R. (2009), "Stability, accuracy and efficiency of sequential methods for coupled flow and geomechanics", *SPE Journal*, Vol. 16 No. 2, pp. 249-262.

Knezevic, M., McCabe, R., Lebensohn, R., Tomé, C. and Mihaila, B. (2012), "Finite element implementation of a self-consistent polycrystal plasticity model: application to uranium", in The Minerals, Metals and Materials Society (Eds), *Supplemental Proceedings: Materials Properties, Characterization and Modeling, Vol. 2*, The Minerals, Metals & Materials Society, Hoboken, NJ, pp. 789-796.

Korzekwa, D.A. (2009), "Truchas – a multi-physics tool for casting simulation", *International Journal of Cast Metals Research*, Vol. 22 No. 4, pp. 187-191.

Kumar, M. and Ghoniem, A.F. (2012a), "Metaphysics simulations of entrained flow gasification. Part I: validating the nonreacting flow solver and the particle turbulent dispersion model", *Energy Fuels*, Vol. 26 No. 1, pp. 451-463.

Kumar, M. and Ghoniem, A.F. (2012b), "Metaphysics simulations of entrained flow gasification. Part II: constructing and validating the overall model", *Energy Fuels*, Vol. 26 No. 1, pp. 464-479.

Larson, J., Jacob, R. and Ong, E. (2005), "The model coupling toolkit: a new fortran90 toolkit for building multi-physics parallel coupled models", *International Journal of High Performance Computer Applications*, Vol. 19 No. 3, pp. 277-292.

Lebensohn, R.A. and Tomé, C.N. (1993), "A self-consistent anisotropic approach for the simulation of plastic deformation and texture development of polycrystals: application to zirconium alloys", *Acta Metallurgica et Materialia*, Vol. 41 No. 9, pp. 611-624.

Leiva, J.S., Blanco, P.J. and Buscaglia, G.C. (2010), "Iterative strong coupling of dimensionally heterogeneous models", *International Journal for Numerical Methods in Engineering*, Vol. 81 No. 12, pp. 1558-1580.

Liang, C., Mahadevan, S. and Sankararaman, S. (2015), "Stochastic multidisciplinary analysis under epistemic uncertainty", *Journal of Mechanical Design*, Vol. 137 No. 2, pp. 021494-1-021404-12.

Lieber, M. and Wolke, R. (2008), "Optimizing the coupling in parallel air quality model systems", *Environmental Modeling and Software*, Vol. 23 No. 2, pp. 235-243.

Lin, H. and Yim, S.C.S. (2006), "Coupled surge-heave motions of a moored system. I: model calibration and parametric study", *Journal of Engineering Mechanics (ASCE)*, Vol. 132 No. 6, pp. 671-680.

Liu, C. and Muraleetharan, K.K. (2012), "Coupled hydro-mechanical elastoplastic constitutive model for unsaturated sands and silts. II: integration, calibration, and validation", *International Journal of Geomechanics (ASCE)*, Vol. 12 No. 3, pp. 248-259.

Matthies, H.G., Niekamp, R. and Steindorf, J. (2006), "Algorithms for strong coupling procedures", *Computer Methods in Applied Mechanics and Engineering*, Vol. 195 No. 17, pp. 2028-2049.

Oliver, T.A., Terejanu, G., Simmons, C.S. and Moser, R.D. (2015), "Validating predictions of unobserved quantities", *Computer Methods in Applied Mechanics and Engineering*, Vol. 283, pp. 1310-1335.

Park, K.C. and Felippa, C.A. (1983), "Partitioned analysis of coupled systems", *Computational Methods in Transient Analysis*, Vol. 1, pp. 157-219.

Rasmussen, C.E. (2004), "Gaussian processes in machine learning", in Bousquet, O., von Luxburg, U. and Rätsch, G. (Eds)*Advanced Lectures on Machine Learning*, Springer, Berlin and Heidelberg, pp. 63-71.

Rizzi, F., Najm, H.N., Debusschere, B.J., Sargsyan, K., Salloum, M., Adalsteinsson, H. and Knio, O.M. (2012), "Uncertainty quantification in MD simulations. Part I: forward propagation", *Multiscale Modeling and Simulation*, Vol. 10 No. 4, pp. 1428-1459.

Roters, F., Eisenlohr, P., Bieler, T.R. and Raabe, D. (2010), *Crystal Plasticity Finite Element Methods in Material Science and Engineering*, John Wiley & Sons.

Rugonyi, S. and Bathe, K.J. (2001), "On finite element analysis of fluid flows fully coupled with structural interactions", *Computer Modeling in Engineering and Sciences*, Vol. 2 No. 2, pp. 195-212.

Sacks, J., Williams, J.T., Mitchell, T.J. and Wynn, H.P. (1989), "Design and analysis of computer experiments", *Statistical Science*, Vol. 4 No. 4, pp. 409-423.

Santner, T.J., Williams, B.J. and Notz, B.I. (2013), *The Design and Analysis of Computer Experiments*, Springer Science & Business Media.

Segurado, J., Lehensohn, R.A., LLorca, J. and Tomé, C.N. (2012), "Multiscale modeling of plasticity based on embedding the viscoplstic self-consistent formulation in implicit finite elements", *International Journal of Plasticity*, Vol. 28 No. 1, pp. 124-140.

Smith, A.F.M. and Roberts, G.O. (1993), "Bayesian computation via the Gibbs sampler and related Markov chain Monte Carlo methods", *Journal of the Royal Statistical Society Series B*, Vol. 55 No. 1, pp. 3-23.

Sorti, M.A., Nigro, N.M., Rodrigo, R.P. and Lisandro, D.D. (2009), "Strong coupling strategy for fluid–structure interaction problems in supersonic regime via fixed point iteration", *Journal of Sound and Vibration*, Vol. 320 No. 4, pp. 859-877.

Steinberg, D.M. (1985), "Model robust response surface designs: scaling two-level factorials", *Biometrika*, Vol. 72 No. 3, pp. 513-526.

Stevens, G.N. and Atamturktur, S. (2015), "Experimental validation and uncertainty quantification of partitioned models", *NAFEMS World Congress*, *San Diego, CA*, *June 21-24*.

Tawhai, M.H. and Bates, J.H.T. (2011), "Multi-scale Lung modeling", *Journal of Applied Physiology*, Vol. 110 No. 5, pp. 1466-1472.

Tomé, C.N., Mauldin, P.J., Lebensohn, R.A. and Kaschner, G.C. (2001), "Mechanical response of zirconium – I. Derivation of a polycrystal constitutive law and finite element analysis", *Acta Materialia*, Vol. 49 No. 15, pp. 3085-3096.

Wang, Y.B., Louie, M., Cao, Y., Liao, X.Z., Li, H.J., Ringer, S.P. and Zhu, Y.T. (2010), "High-pressure torsion induced microstructural evolution in a hexagonal close-packed Zr alloy", *Scripta Materialia*, Vol. 62 No. 4, pp. 214-217.

Williams, C.K. (1998), "Prediction with Gaussian processes: from linear regression to linear prediction and beyond", in Jordan, M.I. (Ed.), *Learning in Graphical Models*, Springer, Dordrecht, pp. 599-621.

Williams, C.K. and Rasmussen, C.E. (2006), *Gaussian Processes for Machine Learning*, *Vol. 2*, No 3, MIT Press.

Xi, Z., Pan, H., Fu, Y. and Yang, R.J. (2014), "A copula-based approach for model bias characterization", *SAE International Journal of Passenger Cars – Mechanical Systems*, Vol. 7 No. 2, pp. 781-786.

Xiong, Y., Chen, W., Kwok-Leung, T. and Apley, D.W. (2009), "A better understanding of model updating strategies in validating engineering models", *Computer Methods in Applied Mechanics and Engineering*, Vol. 198 No. 15, pp. 1327-1337.

Further reading

Atamturktur, S., Hemez, F., Williams, B., Tomé, C. and Unal, C. (2011), "A forecasting metric for predictive modeling", *Computers and Structures*, Vol. 89, pp. 2377-2387.

Boyack, B., Duffey, R., Wilson, G., Griffith, P., Lellouche, G., Levy, S. and Zuber, N. (1989), "Quantifying reactor safety margins: application of code scaling, applicability, and uncertainty evaluation methodology to a large-break, loss-of-coolant accident", Div. of Systems Research, Nuclear Regulatory Commission, Washington, DC.

About the authors

Garrison Stevens is a GAANN Fellow at the Clemson University in the Glenn Department of Civil Engineering. She received her BS and MS in Civil Engineering with a structures emphasis from the Clemson in 2012 and 2014, respectively.

Dr Sez Atamturktur, an Associate Professor at the Clemson University, focusses on the development, application and dissemination of model validation and uncertainty quantification techniques. As principle investigator, Dr Atamturktur has received funding over $3.5 M from US federal and state organizations. Since joining the Clemson, she has graduated nine doctoral students and 11 master students. Along with her research team, Dr Atamturktur has authored more than 70 peer-reviewed scholarly articles, a number of which have received best paper nominations or awards. She is the 2014 recipient of the Murray Stokely Outstanding Teacher award. She regularly receives funded invitations to speak at international conferences and meetings from institutions in countries such as France, Switzerland, Turkey, and Germany. Dr Atamturktur serves as the Chair of the Model Validation and Uncertainty Quantification Technical Division of the Society of Experimental Mechanics and is currently a Guest-Editor for two peer-reviewed journals. Prior to joining the Clemson, Dr Atamturktur served as an LTV Technical Staff Member at the Los Alamos National Laboratory, where she received the LANL Outstanding Contribution Award. Dr Atamturktur received her PhD in Civil and Environmental Engineering from the Pennsylvania State University in 2009. Dr Sez Atamturktur is the corresponding author and can be contacted at: sez@clemson.edu

Dr Ricardo Lebensohn received his PhD Degree in Physics from the University of Rosario, Argentina, in 1993. He joined the Los Alamos National Laboratory, Los Alamos, NM, USA, in

2003. He is currently a Scientist 4 with the Materials Science and Technology Division, working in the field of mechanics of materials, in the area of modeling structure/property relationships of heterogeneous materials (metals, polymers, geomaterials).

Dr George Kaschner received his PhD in Materials Science and Engineering from the University of California, Davis, in 1996. He joined the Los Alamos National Laboratory, Los Alamos, New Mexico, USA, in 1997. He studied mechanical deformation mechanisms and actinides in the Materials Science and Technology Division for 17 years. He is now a Member of Weapon Systems Engineering Division, and works as a System Surveillance Engineer.